Biosensors and Bioelectronics 48 (2013) 108–112

Contents lists available at SciVerse ScienceDirect

Biosensors and Bioelectronics

journal homepage: www.elsevier.com/locate/bios

Aptamer biosensor for label-free impedance spectroscopy detection of potassium ion based on DNA G-quadruplex conformation

Zhengbo Chen*, Liang Chen, He Ma, Tong Zhou, Xiaoxiao Li

Department of Chemistry, Capital Normal University, Beijing 100048, China

ARTICLE INFO

Article history:
Received 1 February 2013
Received in revised form
22 March 2013
Accepted 2 April 2013
Available online 17 April 2013

Keywords:
Aptamer
Electrochemical impedance spectroscopy
Potassium ion
G-quadruplex

ABSTRACT

Herein, a label-free and highly sensitive electrochemical impedance spectroscopy (EIS) aptasensor for the detection of potassium ion (K^+) was developed based on a conformational change in which a K^+-stabilized single stranded DNA (ssDNA) with G-rich sequence was used as the recognition element. In the measurement of K^+ ions, the change in interfacial electron transfer resistance (R_{ct}) of the sensor using a redox couple of $[Fe(CN)_6]^{3-/4-}$ as the probe was monitored. In the presence of K^+, the G-rich DNA folded into the G-quadruplex structure, and then K^+ can bind to the G-quadruplex structure, leading to an increase in the R_{ct}. The R_{ct} increased with K^+ concentration, and the plot of R_{ct} against the logarithm of K^+ concentration is linear over the range from 0.1 nM to 1 mM with a detection limit of 0.1 nM. Other metal ions, such as Ca^{2+}, Mg^{2+}, Na^+, Li^+, Al^{3+}, Zn^{2+}, Cu^{2+}, and Ni^{2+} caused no notable interference on the detection of K^+. The scheme reported herein is applicable to the detection of other kinds of G-rich aptamer-binding chemicals and biomolecules.

1. Introduction

Potassium ions (K^+) exist in extracellular spaces, tissue of animals and plants, biological fluids, and so on (Lippard and Berg, 1994). They play key roles in living organisms, such as nerve transmission, maintenance of muscular strength and extracellular osmolarity, enzyme activation, apoptosis of a cell, regulation of blood pressure and pH, and the concentration of other ions in living cells (Teresa et al., 2000; He et al., 2003; Kuo et al., 2001; Yu et al., 2001; Walz, 2000). Normal serum K^+ levels are between 3.8 and 5.4 mmol/L (Yu et al., 1997). Abnormal K^+ concentrations in biological fluids usually lead to several diseases such as kidney, high blood pressure, stroke, Addison's and adrenal gland diseases (Teixeira et al., 2009; Modesto et al., 2006; Michaud and Strickberger, 2001). Therefore, sensitive K^+-selective sensors are important for the measurement of physiological potassium level to facilitate diagnosis and treatment or to assess water quality affected by agricultural leaching or industrial pollution.

Aptamers are nucleic acid ligands that bind to specific target molecules with high affinity and specificity (Ellington and Szostak, 1990; Tuerk and Gold, 1990; Bruno and Kiel, 1999; Wilson et al., 2001; Hamaguchi et al., 2001). In particular, a single-stranded DNA with guanine (G)-rich sequences can fold into a secondary structure, G-quadruplex, via intramolecular hydrogen-bonding interactions (Davis, 2004; He et al., 2005; Guo et al., 2009). Its formation is known to be promoted by the presence of monovalent cations such as potassium ions (Walmsley and Burnett, 1999). Aptamers possess more advantages over antibodies such as chemical synthesis, selection through the SELEX (systematic evolution of ligands by exponential enrichment) process, easy modification, high stability, target versatility, easy-to-stock, and resistant to denaturation and degradation.

So far, aptasensors for K^+ detection have been developed based on different technologies, including flame atomic absorption spectrometry (Jesus et al., 2008), ion chromatography (Zhou et al., 2007), surface plasmon resonance (Chen et al., 2008), fiber optic sensors (Wygladacz and Bakker, 2005; Ertekin et al., 2002; Krause et al., 1998), fluorescence spectrum (Liu et al., 2011; Hirata et al., 2011; Shi et al., 2010; Fan et al., 2012; Kong et al., 2009a, 2009b; Yuanboonlim et al., 2012) and electrochemical method (Wu et al., 2008; Ge et al., 2010; Nguyen et al., 2009; Teixeira et al., 2009). Among these techniques, the electrochemical methods play important roles in the development of aptasensors due to their high sensitivity, fast response, simple instrumentation, low production cost, and portability.

Electrochemical impedance spectroscopy (EIS) is a rapidly developing electrochemical technique for the investigation of bulk and interfacial electrical properties of any kind of solid or liquid material which is connected to, or part of, an appropriate electrochemical transducer (Katz and Willner, 2003). Any intrinsic property of a material or a specific process that can affect the interfacial properties of an electrochemical system can potentially be studied by EIS (Bard and Faulkner, 1980; McDonald, 1987).

* Corresponding author. Tel.: +86 1068903047.
E-mail address: czb979216@sina.com (Z. Chen).

0956-5663/$ - see front matter © 2013 Elsevier B.V. All rights reserved.
http://dx.doi.org/10.1016/j.bios.2013.04.007

EIS apsensors, which are based on the change of electron transfer resistance using a redox probe couple such as $[Fe(CN)_6]^{3-/4-}$, possess unique advantages, such as ease of signal quantification, an ability to separate the surface binding events from the solution impedance, and less destruction to the biological interactions being measured, and most importantly, redox marker-free on the DNA strand (Li et al., 2008; Bogomolova et al., 2009; Chen et al., 2011).

Herein, we describe a simple, label-free electrochemical impedimetric aptasensor for detection of K^+ based on G-quadruplex structures. It is also known that a G-quadruplex has a channel at its center with a diameter that correlates well with the ionic radius of K^+ (1.3 Å; Kong et al., 2009a, 2009b). The immobilization of the recognition element (anti-K^+ aptamer) introduces electrical insulation and kinetic-transfer barriers at the electrode surface. The transduction principle is based on electron transfer resistances in the presence of an $[Fe(CN)_6]^{3-/4-}$ redox couple. It is known that the K^+ ion can promote the conversion of a G-rich sequence from a loose random coil into a compact G-quadruplex. G-quaduplex DNA has a much higher space charge density than ssDNA. So the aptamer-K^+ interaction leads to an increase in the electron transfer resistance, repelling the redox marker ions to approach the electrode, which can be measured by electrochemical impedance spectroscopy. The result indicates that the values of R_{ct} have a very good linear relationship with the logarithm of K^+ concentration over the range from 0.1 nM to 1 mM with a detection limit of 0.1 nM. The EIS aptasensor demonstrated here is very simple, cost-effective, extremely sensitive and highly specific, especially, it is label-free, and requires no external modification on the biomolecules.

2. Experimental

2.1. Apparatus and reagents

An advanced electrochemical system (Princeton Applied Research (PARSTAT 2273)) was used for the electrochemical measurements. All experiments were performed using a conventional three-electrode system with a fabricated aptasensor or bare gold (diameter, 2 mm) as the working electrode, Ag/AgCl (sat. KCl) as the reference electrode, and a platinum as counter electrode. All potentials were referred to the reference electrode.

The single strand DNA oligonucleotide was synthesized by TaKaRa Biotechnology (Dalian, China) Co., Ltd. The sequence of oligonucleotide employed is: 5′-TTTGGTTGGTGTGGTTGGTTT-3′-$(CH_2)_6$–SH. Tris-(2-carboxyethyl) phosphine hydrochloride (TCEP) was obtained from the Alfa Aesar (Tianjing) company. Tris-base was purchased from Sigma-Aldrich.

All other reagents are of analytical reagent grade. All solutions were prepared with double distilled water. Immobilization buffer (20 mM Tris–HCl, pH 7.41) containing 10 mM $Na_3Fe(CN)_6/Na_4Fe(CN)_6$ was chosen as the supporting electrolyte for K^+.

2.2. Fabrication of the aptasensor

First, gold substrates were cleaned by immersion in a 3:1 mixture of concentrated H_2SO_4 and 30% H_2O_2 (piranha) for 5 min at 90 °C (Kawde et al., 2005), followed by rinsing with copious amounts of deionized water. Next, the electrode was polished with 1, 0.3 and 0.05 μm malumina powders, followed by sonication in ethanol and deionized water, and electrochemical cleaning (a series of oxidation and reduction cycles in 0.5 M H_2SO_4 with the potential between −0.2 and +1.5 V at 0.1 V/s), until a representative cyclic voltammogram of a clean gold electrode was obtained. Then, the 10 μL droplet of anti-K^+ aptamer (1 μM) was placed on the gold electrode surface for 20 h at 100% humidity for later electrochemical analysis. Prior to the use of the anti-K^+ aptamer, the aptamer (1 μM) including 1 mM TCEP in Immobilization buffer which was used to reduce disulfide bond oligos was heated to 90 °C for 5 min and then gradually cooled to room temperature. This heating and cooling step helps to maintain the structural flexibility of the aptamer. For K^+ assays, the aptamer-modified electrode was placed into 2 mL K^+ solutions of various concentrations.

3. Results and discussion

3.1. Sensing mechanism of the aptasensor

A schematic representation of aptasensor with fabrication steps and performance is displayed in Fig. 1. On exposure of the anti-K^+ aptamer modified electrode to an Immobilization buffer containing $[Fe(CN)_6]^{3-/4-}$, which serves as a signaling transducer the negatively-charged aptamer probe acts as an electrostatic barrier that repelled the $[Fe(CN)_6]^{3-/4-}$ marker and hinders its interfacial electron transfer reaction (Yu et al., 2003). After K^+ was added to the electrochemical cell, the aptamer part bounded to K^+ and folded to a G-quaduplex structure. G-quaduplex DNA has a much higher space charge density than ssDNA, because the persistence length of random coil ssDNA with 21 bases is about 8.7 nm and that of more condensed G-quaduplex DNA is only about 1.5 nm, while they possess the same charge numbers. So the G-quaduplex structure results in less availability for a redox reaction.

3.2. Performance of the aptasensor

To quantitatively assess the detection limit and response range of the K^+ aptasensor, Fig. 2A shows the Nyquist plots of aptamer/gold electrode for K^+ with different concentrations. The impedance spectrum consists of a semi-circle at high frequencies, and a straight line at low frequencies. Owing to the double-layer capacitance (C_{dl}) and the charge-transfer resistance (R_{ct}), the semi-circle can be found at high frequencies. But when the frequencies come to low frequencies, the Warburg diffusion is the most important factor, which exhibits the straight line of 45°

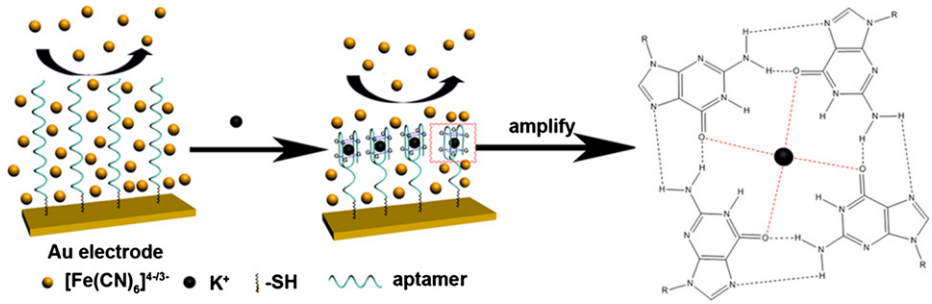

Fig. 1. Schematic illustration of the label-free EIS sensing of K^+ at the aptamer-modified gold electrode.

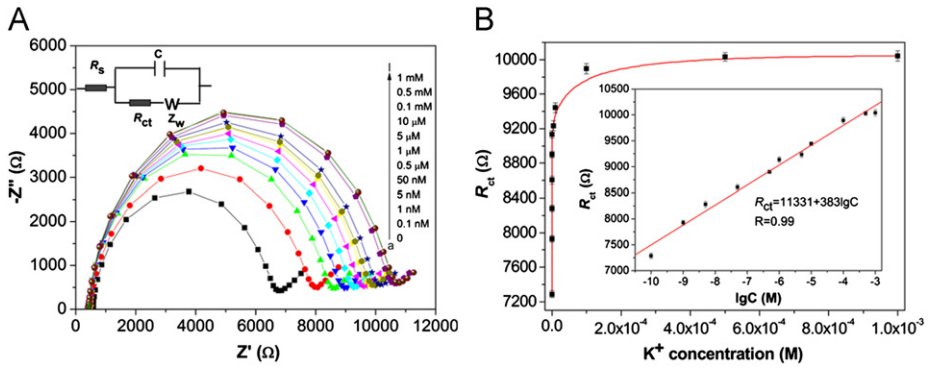

Fig. 2. (A) Nyquist plots of the aptamer/gold electrode after interaction with different concentrations of K^+ (a) 0, (b) 0.1 nM, (c) 1 nM, (d) 5 nM, (e) 50 nM, (f) 0.5 μM, (g) 1 μM, (h) 5 μM, (i) 10 μM, (j) 0.1 mM, (k) 0.5 mM, and (l) 1 mM. The biased potential was 0.192 V vs Ag–AgCl, the frequency was from100 kHz to 100 mHz and the amplitude was 10.0 mV. The inset shows a Randle modified equivalent circuit. (B) The dependence of R_{ct} of the aptamer/gold electrode on the concentration of K^+. The inset shows the R_{ct} is linear with logarithm of K^+ concentration over the range from 0.1 nM to 1 mM.

Table 1
Values of the equivalent circuit parameters of the fitting curves.

Number unit	C (M)	R_s (ohm cm^2)	Z_{CPE} (S s^n/cm^2)	n (1)	R_{ct} (ohm cm^2)	Warburg (S s^5/cm^2)
1	0	562.9	7.75×10^{-7}	0.9244	5998	0.00104
2	1.00×10^{-10}	470.1	7.38×10^{-7}	0.9087	7287	0.00094
3	1.00×10^{-9}	434.0	7.79×10^{-7}	0.9263	7925	0.00118
4	5.00×10^{-9}	442.0	7.80×10^{-7}	0.9274	8281	0.00118
5	5.00×10^{-8}	443.6	7.97×10^{-7}	0.9271	8604	0.00117
6	5.00×10^{-7}	438.2	8.18×10^{-7}	0.9259	8901	0.00117
7	1.00×10^{-6}	439.6	8.19×10^{-7}	0.9269	9134	0.00118
8	5.00×10^{-6}	430.8	8.29×10^{-7}	0.9261	9234	0.00117
9	1.00×10^{-5}	434.8	8.36×10^{-7}	0.9264	9442	0.00118
10	1.00×10^{-4}	430.9	8.52×10^{-7}	0.9264	9895	0.00115
11	5.00×10^{-4}	431.7	8.54×10^{-7}	0.9275	10030	0.00115
12	1.00×10^{-3}	426.6	8.60×10^{-7}	0.928	10040	0.00113

(Radi et al., 2005). From curve *a* to *l* (Fig. 2A), owing to the increase of the charge-transfer resistance (R_{ct}), the radius of the semi-circle becomes bigger. In view of the dispersion effect of the system, we replaced the double-layer capacitance with constant phase element (CPE).

$$Z_{CPE} = \frac{1}{Y_0}(j\omega)^{-n}$$

The system can be modeled using the Randles circuit (inset of Fig. 2A). The impedance spectrum is fitted by the software ZSimpWin (Copyright@1999-2002 EChem software. Author: Bruno Yeum, PdD). The result of the fitting is shown in Table 1. By the software, the parameters were calculated and the dependence of R_{ct} on the concentration of K^+ (0.1 nM–1 mM) was as shown in Fig. 2B. We can see that R_{ct} increases dramatically when the concentration is below 0.5 mM. Subsequently, the R_{ct} reaches a plateau, presuming that at first, there are a lot of active sites at the electrode surface, the concentration of the solute (K^+) is low, the solute from the solution can be timely absorbed by these active sites. However, with the increase of concentration of the solute, the former sites binding with the solute hinder the latter solute, or say, the solute which will bind to aptamer is influenced by the steric hindrance of the binding site previously, leading to repulsion of aptamer with G-quaduplex structure to the subsequent K^+. This is somewhat similar to the Temknh adsorption isotherm model. We found that R_{ct} is linear with logarithm of K^+ concentration over a range from 0.1 nM to 1 mM, as shown in the inset of Fig. 2B; the regression equation is R_{ct}=11331+383 log C (unit of C is M) and the regression coefficient (r) is 0.994. According to the fitting equation, the R_{ct} values of the last two points are almost equal. This means that the reactive sites which can react with solute nearly saturated at the electrode. The directly measured limit of this method for K^+ is 0.1 nM (evaluated by the actually EIS response as the lowest concentration of K^+ that can be distinguished at a stated level of probability from the blank solutions). The relative standard deviation for results from the DNA duplex/gold electrode for each K^+ concentration, are listed in Table S1. These indicate that the proposed biosensor offers excellent reproducibility (RSDs < 0.74%, n=3). In addition, to show the advantages of our proposed sensor, a comparison table of the performances with different K^+ aptasensors is shown below. From Table 2, it can be seen that the detection limit of our proposed sensor (0.1 nM) is better than most analogical aptasensors and the linear range of our work is relatively wide.

3.3. Selectivity of the proposed aptasensor

Not only does the aptasensor has to be sensitive to different concentrations of the analyte, also it must be specific. The specificity of the sensor was determined by challenging it with other metal ions as shown in Fig. 3A and B. As expected, the R_{ct} of the aptasensor had little changes after treatment with 0.1 mM Ca^{2+}, Mg^{2+}, Na^+, Li^+, Al^{3+}, Zn^{2+}, Cu^{2+}, and Ni^{2+} compared with that obtained without containing K^+. However, after the addition of 0.1 mM K^+, a significant enhancement of the R_{ct} was obtained, indicating that the response of the sensor to K^+ was unaffected by presence of other metal ions. Otherwise, as we know, human urine sample contains other commonly found constituents, which was used as interfering compounds to further confirm the selectivity of the proposed sensor toward K^+. The urine sample containing 15 mM was taken from Peking University Third Hospital. When the R_{ct} of the proposed system was measured in the presence of

Table 2
Comparison between the proposed assay and other reported techniques for the determination of K^+.

Method	Technique	LOD	Linear range	References
Electrochemical	EIS	0.1 nM	0.1 nM–1 mM	This work
Electrochemical	CV[a]	20 nM	50 nM–0.7 mM	Nguyen et al., 2009
Electrochemical	Potentiometric	72.7 μM	12.6 μM–1.62 mM	Teixeira et al., 2009
Optical	Fluorescence	1.5 nM	5–30 nM	Kim et al., 2012
Optical	Fluorescence	0.9 μM	4 μM–1 mM	Yuanboonlim et al., 2012
Optical	RSSA[b]	0.5 nM	0.06–3350 μM	Cai et al., 2010
Optical	Fluorescence	0.4 mM	0.6–20 mM	Shi et al., 2010
Optical	Fluorescence	0.005 mM	0.005–1 mM	Liu et al., 2011
Optical	Fluorescence	2.5 μM	2.5 μM–5 mM	Fan et al., 2012

[a] Cyclic voltammetry.
[b] Resonance scattering spectral assay.

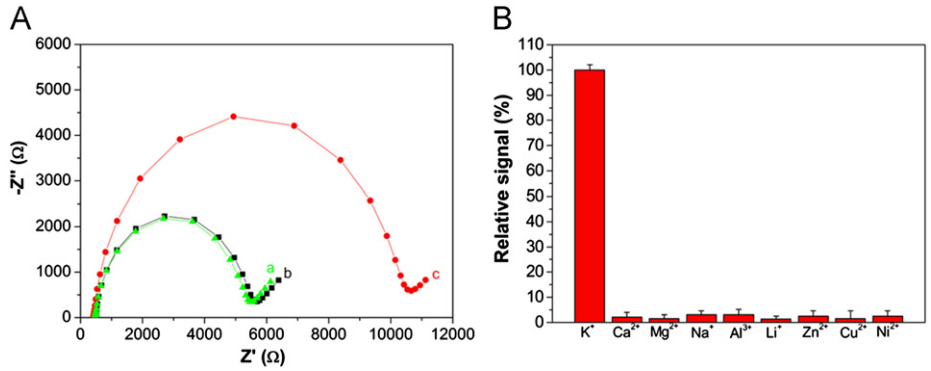

Fig. 3. (A) Nyquist plots of impedance spectra for the aptamer/gold electrode after reaction with (a) 0 M K^+, (b) 0.1 mM Ca^{2+}, Mg^{2+}, Na^+, Al^{3+}, Li^+, Zn^{2+}, Cu^{2+} and Ni^{2+} and (c) a mixture of 0.1 mM K^+, Ca^{2+}, Mg^{2+}, Na^+, Al^{3+}, Li^+, Zn^{2+}, Cu^{2+} and Ni^{2+}. (B) Relative response for aptamer-modified electrode after reaction with various ions (all at 0.1 mM).

urine sample, the R_{ct} increased dramatically compared to blank solution (without K^+), with addition of various ions other than K^+, the R_{ct} had almost no changes. It was obvious that the method has high selectivity for K^+.

3.4. Application of the aptasensor

The sensor was further applied to perform K^+ assay in real human urine samples. As we know, the level of K^+ in urine is indicative of certain kidney diseases and the normal concentration of K^+ in the urine is in the range of 25–125 mM (Huang and Chang, 2008). We filtered the urine samples from four healthy volunteers through 0.2 mm membrane, and then diluted the samples 100-fold using deionized water. The K^+ concentrations in the four urine samples detected by the proposed strategy were 32 mM, 45 mM, 115 mM, 108 mM, respectively, and the values were in the normal range of K^+ in the urine. In addition, a 100-fold diluted urine sample to which known amounts of K^+ were added was investigated by spike and recovery experiments, and the recovery of standard addition was in the range of 91.16–100.70%. The experimental results confirmed the effectiveness of this method for determination of K^+ content in real samples.

4. Conclusions

In conclusion, a simple, sensitive and label-free EIS aptasensor was developed for the detection of K^+, in which G-rich DNA was used as a K^+ recognition element, and $[Fe(CN)_6]^{3-/4-}$ as a redox probe. The method demonstrated a linear relationship with the concentration of K^+ ranging from 0.1 nM to 1 mM, and a detection limit of 0.1 nM was achieved. In addition, it also exhibited remarkably high sensitivity, repeatability and selectivity. This work also demonstrated that EIS method was an efficient method for the study of aptamer-metal ions interfacial interactions on gold electrode. This protocol is still promising for broad potential applications in clinical assay.

Acknowledgments

This work was financially supported by Dr. Start-Up Capital.

Appendix A. Supporting information

Supplementary data associated with this article can be found in the online version at http://dx.doi.org/10.1016/j.bios.2013.04.007.

References

Bard, A.J., Faulkner, L.R., 1980. Electrochemical Methods: Fundamental and Applications. Wiley, New York.
Bogomolova, A., Komarova, E., Reber, K., Gerasimov, T., Yavuz, O., Bhatt, S., et al., 2009. Analytical Chemistry 81, 3944–3949.
Bruno, J.G., Kiel, J.L., 1999. Biosensors and Bioelectronics 31, 457–464.
Cai, W., Fan, Y.Y., Jiang, Zhiliang, Yao, J.N., 2010. Talanta 81, 1810–1815.
Chen, H., Gal, Y.S., Kim, S.H., 2008. Sensors and Actuators B: Chemical 133, 577–581.
Chen, Z.B., Li, L.D., Zhao, H.T., Guo, L., Mu, X.J., 2011. Talanta 83, 1501–1506.
Davis, J.T., 2004. Angewandte Chemie International Edition 43, 668–698.
Ellington, A.D., Szostak, J.W., 1990. Nature 346, 818–822.
Ertekin, K., Tepe, M., Yenigul, B., 2002. Talanta 58, 719–727.
Fan, X.Y., Li, H.T., Zhao, J., Lin, F.B., Zhang, L.L., Zhang, Y.Y., et al., 2012. Talanta 89, 57–62.
Ge, B.X., Huang, Y.C., Sen, D., Yu, H.Z., 2010. Angewandte Chemie International Edition 49, 9965–9967.
Guo, J.H., Zhu, L.N., Kong, D.M., Shen, H.X., 2009. Talanta 80, 607–613.
Hamaguchi, N., Ellington, A., Stanton, M., 2001. Analytical Biochemistry 294, 126–131.

He, F., Tang, Y., Wang, S., Li, Y., Zhu, D., 2005. Journal of the American Chemical Society 127, 14286–14287.
He, H., Mortellaro, M.A., Leiner, M.J.P., Fraatz, R.J., Tusa, J.K., 2003. Journal of the American Chemical Society 125, 1468–1469.
Hirata, T., Terai, T., Komatsu, T., Hanaoka, K., Nagano, T., 2011. Bioorganic and Medicinal Chemistry 21, 6090–6093.
Huang, C.C., Chang, H.T., 2008. Chemical Communications, 1461–1463.
Jesus, A., Silva, M.M., Vale, M.G.R., 2008. Talanta 74, 1378–1384.
Katz, E., Willner, I., 2003. Electroanalysis 15, 913–947.
Kawde, A.N., Rodriguez, M.C., Lee, T.M.H., Wang, J., 2005. Electrochemistry Communications 7, 537–540.
Kim, B., Jung, I.H., Kang, M., Shim, H.K., Woo, H.Y., 2012. Journal of the American Chemical Society 134, 3133–3138.
Kong, D., Ma, Y., Guo, J., Yang, W., Shen, H., 2009a. Analytical Chemistry 81, 2678–2684.
Kong, D.M., Guo, J.H., Yang, W., Mab, Y.E., Shen, H.X., 2009b. Biosensors and Bioelectronics 25, 88–93.
Krause, C., Werner, T., Huber, C., 1998. Analytical Chemistry 70, 3983–3985.
Kuo, H.C., Cheng, C.F., Clark, R.B., Lin, J.J.C., Lin, J.L.C., Hoshijima, M., et al., 2001. Cell 107, 801–813.
Li, X.X., Shen, L.H., Zhang, D.D., Qi, H.L., Gao, Q., Ma, F., Zhang, C.X., 2008. Biosensors and Bioelectronics 23, 1624–1630.
Lippard, S.J., Berg, J.M., 1994. Principles of Bioinorganic Chemistry. University Science Books, Mill Valley, CA.
Liu, Y.Y., Li, B.X., Cheng, D.M., Duan, X.Y., 2011. Microchemical Journal 99, 503–507.
McDonald, J.R., 1987. Impedance Spectroscopy: Emphasizing Solid Materials and Systems. Wiley, New York.
Michaud, G.F., Strickberger, S.A., 2001. Journal of the American College of Cardiology 38, 1224–1225.
Modesto, K.M., Møller, J.E., Freeman, W.K., Shub, C., Bailey, K.R., Pellikka, P.A., 2006. American Journal of Cardiology 97, 1247–1249.
Nguyen, B.T.T., Ang, J.Q., Toh, C.S., 2009. Electrochemistry Communications 11, 1861–1864.
Radi, A.E., Sanchez, J.L.A., Baldrich, E., O'Sullivan, C.K., 2005. Analytical Chemistry 77, 6320–6323.
Shi, C., Gu, H.X., Ma, C.P., 2010. Analytical Biochemistry 400, 99–102.
Teixeira, M.F.S., Freitas, B.H., Seraphim, P.M., Salmazo, L.O., Nobrea, M.A., Lanfredi, S., 2009. Procedia Chemistry 1, 293–296.
Teresa, M., Gomes, S.R., Tavares, K.S., Oliveira, J., 2000. Analyst 125, 1983–1986.
Tuerk, C., Gold, L., 1990. Science 249, 505–510.
Walmsley, J.A., Burnett, J.F., 1999. Biochemistry 38, 14063–14068.
Walz, W., 2000. Neurochemistry International 36, 291–300.
Wilson, D.S., Keefe, A.D., Szostak, J.W., 2001. Proceedings of the National Academy of Science USA 98, 3750–3755.
Wu, Z.S., Chen, C.R., Shen, G.L., Yu, R.Q., 2008. Biomaterials 29, 2689–2696.
Wygladacz, K., Bakker, E., 2005. Analytica Chimica Acta 532, 61–69.
Yu, B., Nie, L., Yao, S., 1997. Journal of Chromatography B 693, 43–49.
Yu, H.Z., Luo, C.Y., Sankar, C.G., Sen, D., 2003. Analytical Chemistry 75, 3902–3907.
Yu, S.P., Canzoniero, L.M.T., Choi, D.W., 2001. Current Opinion in Cell Biology 13, 405–411.
Yuanboonlim, W., Siripornnoppakhun, W., Niamnont, N., Rashatasakhon, P., Vilaivan, T., Sukwattanasinitt, M., 2012. Biosensors and Bioelectronics 33, 17–22.
Zhou, B., Zhang, L., Zhang, G., 2007. Journal of Chromatography B 852, 278–281.